

JET-P(87)21

J. Jacquinot, V.P. Bhatnagar, G. Bosia, M. Bures, G.A. Cottrell, Ch. David,
M.P. Evrard, D. Gambier, C. Gormezano, T. Hellsten, A.S. Kaye, S. Knowlton,
D. Moreau, F. Sand, D.F.H. Start, P.R. Thomas, K. Thomsen and T. Wade

Results of RF Heating on JET and Future Prospects

Results of RF Heating on JET and Future Prospects

J. Jacquinot¹, V.P. Bhatnagar², G. Bosia¹, M. Bures¹, G.A. Cottrell¹, Ch. David³,
M.P. Evrard², D. Gambier³, C. Gormezano¹, T. Hellsten¹, A.S. Kaye¹, S. Knowlton⁴,
D. Moreau¹, F. Sand¹, D.F.H. Start¹, P.R. Thomas¹, K. Thomsen¹ and T. Wade¹

JET-Joint Undertaking, Culham Science Centre, OX14 3DB, Abingdon, UK

¹*JET Joint Undertaking, Abingdon, Oxon, OX14 3EA, UK*

²*EUR-EB Association, LLP-ERM/KMS, B-1040 Brussels, Belgium*

³*EUR-CEA Association, CEN Cadarache, France*

⁴*Plasma Fusion Centre, MIT, Cambridge, Mass. USA*

“This document contains JET information in a form not yet suitable for publication. The report has been prepared primarily for discussion and information within the JET Project and the Associations. It must not be quoted in publications or in Abstract Journals. External distribution requires approval from the Publications Officer, JET Joint Undertaking, Abingdon, Oxon, OX14 3EA, UK”.

“Enquiries about Copyright and reproduction should be addressed to the Publications Officer, EFDA, Culham Science Centre, Abingdon, Oxon, OX14 3DB, UK.”

The contents of this preprint and all other JET EFDA Preprints and Conference Papers are available to view online free at www.iop.org/Jet. This site has full search facilities and e-mail alert options. The diagrams contained within the PDFs on this site are hyperlinked from the year 1996 onwards.

RESULTS OF RF HEATING ON JET AND FUTURE PROSPECTS

ABSTRACT

Ion Cyclotron Resonance Heating (ICRH) has been applied to various JET plasmas with net coupled powers reaching 7 MW for several seconds. Conditioning with helium discharges is shown to be effective in controlling the density and in reducing the total radiated power to about 25% of the input power. On axis heating invariably results in long sawteeth of large amplitude. In most high power cases, a sudden bifurcation to monster sawteeth as long as 1.6 s is observed. The monster sawtooth is accompanied by an improvement in energy confinement time (+20%) and by an increase in density. Central electron and ion temperatures of 7 and 5.5 keV respectively have been achieved with 6.5 MW of ICRF power. The heating rate is reduced with off-axis heating in agreement with diffusive heat transport models.

The future RF programme on JET includes upgrading the ICRF power to 20 MW and the development of current drive methods using a phased ICRF array of 8 antennae and later on a Lower Hybrid Current Drive system at 3.7 GHz with a 10 MW launcher.

1. INTRODUCTION The JET RF programme now consists of two distinct activities:

(i) Ion Cyclotron Resonance Heating (ICRH), which started operation in 1985. The first stage of this programme has recently been completed.

(ii) Lower Hybrid Current Drive (LHCD). Studies started in 1986 and approval for the construction of a first stage of the 3.7 GHz equipment has been obtained.

ICRH and NBI will ultimately (c. 1988) inject 40 MW of power in the plasma (20 MW each). LHCD is aimed at controlling the current profile in order to suppress the sawteeth and possibly to achieve higher confinement regimes.

This article, which follows several previous reports [1a, b, c,], summarizes the main experimental results obtained with ICRH.

Power accountability has been deduced from the stored energy response to a step power increase [1a]. The power deposition profile has been analysed using power modulation of long pulses [1c].

As expected in large Tokamaks with short antennae located near the equatorial plane about 80% of the power is deposited in a narrow zone (± 10 cm for off-axis heating, ± 30 cm for on-axis heating) defined by the iou-iou hybrid resonance. The 20% remaining power seems to appear at the edge producing serious modifications of the scrape off layer. These edge effects can be suppressed by phasing coupling elements toroidally [3] so that most of the power is radiated at a high $k_{//}$ ($\approx 7 \text{ m}^{-1}$). The heating rate in this case was higher (+ 25%) presumably because all the power was now available for plasma core heating. These experiments were limited to low power (~ 1.5 MW) due to a low coupling resistance but suggested a redesign of the antennae to allow this mode of operation with improved coupling for the next stage of the ICRH programme.

Earlier plasma heating studies [1a,b,4] have shown that the increase of plasma stored energy is rather insensitive to the method of heating (ICRH, NBI). More extensive studies have demonstrated the interest of local heating [1b,c,5] in the plasma centre due to the diffusive nature of heat transport [5]. Another major difference between NBI and ICRF using a minority species is that NBI dominantly heats the ions and ICRF heats the electrons via a highly energetic minority. At low density NBI creates a "hot ion" mode and ICRF a "hot electron" mode.

This article is organized in the following manner. The ICRF data base is first presented with particular attention to the localisation of the heating zone and to conditions of very low plasma radiation. The resulting scaling of confinement with plasma current is discussed. We then compare the various heating scenarios using the same plasma current but different minority species or magnetic configuration (in particular X-point). Finally we discuss future prospects of RF in JET examining specific RF scenarios capable of producing a high fusion yield without significant activation.

2. EXPERIMENTAL CONDITIONS, HELIUM CONDITIONING Experiments were performed with 3 antennae, all phased (unless stated) in the toroidal monopole mode (e.g. with a radiation spectrum peaked at $k_{//}=0$). Operation just after the installation of the antennae resulted in a high fraction of plasma radiation (e.g. $p = P_{\text{rad}}/P_{\text{tot}} \approx 0.7$) of the input power. The density increase with RF was high and density disruption would set a RF power limit at low plasma current. The situation improved remarkably with high current, high power pulses which apparently carbonized the interior of the vessel. However, p stayed above 0.5 (Fig 1). Discharges in Helium were performed at the end of the operating period. The increase of density with RF was low e.g. no more than 25% for $P_{\text{RF}} = 7$ MW and p decreased from typically 0.55 with ohmic heating to 0.25 at maximum RF power (7.4 MW). These improved conditions remain unchanged after a return to Deuterium plasmas. Fig. 1 illustrates the effect of Helium conditioning for 2 MA plasmas both with Deuterium and Helium species.

3. SCALING OF ENERGY CONFINEMENT WITH ICRF Figs. 2 and 3 summa-

alize the available confinement data of plasmas heated by ICRF heating alone using outboard limiters (in one series of experiments the outboard limiters were removed and the plasma was limited by the side protections of the 3 antennae). The plasma current was varied from 1 MA to 5 MA. This scan was normally done with a constant ratio of the wave frequency to the vacuum toroidal field (ν/B_ϕ). Paramagnetic shift of the resonance (R_c) resulted in a variation of the resonance layer (as much as 25 cm). Fig. 2 gives the stored energy for all limiter discharges with $|R_o - R_c| < 0.55$ m. Note that on axis heating of 5 MA plasmas have only been performed with a 50 cm displacement of the resonance layer. In Fig. 3 the incremental confinement $\tau_{inc} = \Delta W / \Delta P_{tot}$ is plotted for the entire data set as a function of the resonance position. For each data subset the heating efficiency decreases as the resonance is moved out. The data is well represented by a law

$$\tau_{inc} = \tau_o (1 - (r_c/a)^2)^2 ; r_c = R_c - R_o \quad (1)$$

This result has now been obtained in the following conditions: (i) in a single shot by ramping down the toroidal magnetic field during the pulse [1b]; (ii) by changing the frequency from shot to shot [1c], (iii) as in (ii) but in Helium discharges with Hydrogen minority heating. In this third series of experiments, the total radiated power was a factor 2 to 3 smaller than in the two other series. The fact that the $\tau_{inc} (r_c/a)$ is similar in all these series despite significant changes in radiation, suggests this data should be analyzed in terms of heat transport models.

Rebut et al [6] have proposed an anomalous transport model in which the heat flux can be described by

$$q = n \chi (VT - VT_c) H (VT - VT_c) \quad (2)$$

Here, the anomalous heat diffusivity χ is "switched on" by the step function H when the electron temperature gradient VT rises above a critical value VT_c .

Callen, et al [5] have analysed in detail the consequences of general diffusion laws and shown that Eq. (2) belongs to a functional form which best represents the following phenomenae observed with additional heating:

(i) the heat pulse propagates with a velocity independent of additional heating power [12];

(ii) the off-set linear law of $W = W_o + \tau_{inc} P$ which is a direct consequence of Eq. (2) assuming that χ does not have a strong dependence on VT. The 2 MA data in Fig 2 is a good illustration of the offset linear law;

(iii) the decrease of heating efficiency with off-axis ICRF heating. Calculations [5] shows that Eq. (1) is obtained provided that χ is assumed to be independent of VT but increases with radius approximately as

$$\chi(r) = \chi_o / (1 - r^2/a^2) \quad (3)$$

We now use Eq. (1) and the off-set linear law to deduce, experimentally, the importance of the plasma current. We write:

$$W = W_0 + \tau_0 P_{tot}^* ; P_{tot}^* = 0.85 P_{OH} + (1-r_c^2/a^2)^2 P_{RF} \quad (4)$$

P_{tot}^* draws its significance from the diffusive heat transport model: P_{tot}^* is the power which when deposited entirely on axis would give the same increase in W as the spatially distributed P_{OH} and the off-axis P_{RF} .

Representation of the data versus P_{tot}^* (Fig 2) shows that:

for 2 MA ; $\tau_0 = 180$ ms, $W_0 = 0.55$ MJ

for 5 MA ; $\tau_0 = 310$ ms, $W_0 = 1.45$ MJ

Using the diffusive heat transport model, it is also possible to correct P_{tot}^* for radiation losses. Including the full profile effects of the radiation following the prescription of [5], we find no changes of τ_0 and W_0 in the 2 MA data but in 5 MA it amounts to a 10% reduction of P_{tot}^* ($\tau_0 = 340$ ms).

A consequence of Eq. (2) is a relation between an averaged critical gradient VT_c and W_0 : $VT_c \approx W_0/2\pi R_0 a^3 n$. We find that $VT_c = 1.7$ keV $m^{-1} \pm .4$ for both the 2 MA and 5 MA data.

The physical significance of the critical gradient VT_c is the expectation of a reduced heat transport in regions where $VT < VT_c$. Such a situation can arise with high power off-axis ICRH. Indeed the heat transport coefficient appear significantly reduced for this case [7]. The reduction concerns only the central zone located inside the heated shell and the overall effect is a loss of heating efficiency.

4. HEATING SCENARIOS, MONSTER SAWTEETH, X-POINT DISCHARGES Recent high power experiments confirm previous conclusions that there is hardly any observable differences in stored energy between scenarios using a He³ or a H minority. In agreement with minority slowing down physics [8], He³ minority heating, particularly at low or moderate power, is more efficient at heating ions than the H minority but at the expense of a smaller electron heating rate. Using high power on-axis heating with $n_{H,He^3}/n_D \approx 0.05$, electron heating via the minority species dominates. The ions are slowly heated by electron collisions. An example of this delayed heating is apparent on Fig. 4.

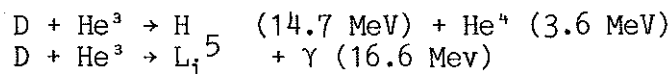
A common feature of high power on-axis heating is the sudden transition [9] from the regular sawteeth behaviour (period ≈ 300 ms) to long MHD quiescent periods of up to 1.6 s ("Monster" sawteeth). The electron temperature (Fig 4) saturates after 200 ms but the density, the stored energy (Fig 5), and the ion temperature keep increasing during the quiescent period. The monster has beneficial effects (gain of a factor of 2 to 3 on the reaction rate and of $\approx +20\%$ on the stored energy). However, its crash may induce a locked MHD mode which deteriorates confinement. In several cases this mode lasted for the rest of the pulse.

On the contrary when the resonance is located outside the $q=1$ surface the sawteeth become smaller and shorter [1b].

ICRF heating of single null X-point discharges has only been performed at 2MA with $P_{RF} < 6\text{MW}$ and 6cm separating the antenna from the plasma (Figs. 4 and 5). No clear transition to an "H mode" regime has been observed. However, the confinement is better than in limiter discharges with the same plasma current. τ_{inc} reaches 350 ms and the confinement degradation is small. The edge MHD activity is smaller than in limiter discharge. This improvement of energy confinement is also accompanied by increased impurity levels. The total radiated power fraction p increases from 0.25 (limiter) to 0.5 (X-point) and Z_{eff} from 2.5 (limiter) to 4.5 (X-point).

5. ICRF SCENARIOS PRODUCING A HIGH YIELD OF D-He³ FUSION REACTIONS

In this section, we consider ICRH scenarios capable of producing a significant amount of fusion yield from non thermal reactions between energetic Deuterium and Helium3 ions. The basic reactions are



The second reaction only occurs with a much smaller probability and is mentioned here as a diagnostic of the process since the γ production can be monitored [10]. The cross-sections for both reactions have maxima at 440 keV. We are interested in producing a significant number of these reactions in order to study the confinement of fusion products without large neutron activation of the Tokamak.

The following ICRF scenarios have been considered:

(S1) He³ minority heated by ICRF in a D plasma, a standard JET operating regime.

(S2) Harmonic Deuterium heating, $2\omega_{CD}$, in a He³ plasma with NBI. In this scenario, the parameters are optimized to maximize the damping of ICRF on the Deuterium beam ions to increase their energy, to the optimum of the D-He³ cross section. Fundamental damping on a H minority is to be avoided in this scheme and therefore an H concentration smaller than 1% is required. In preliminary studies [11] up to 10% of the RF power was absorbed in this manner as deduced from observed beam acceleration above the injection energy.

(S3) $2\omega_C$ He³ scenarios in a D plasma. The 2nd harmonic damping of He³ will become a dominant process when the ion temperature reaches 7 keV. This will be best achieved in the hot ion mode generated by NBI at low or moderate densities. Again in this scheme, fundamental damping by an H minority can occur on the high field side of the Tokamak, and thorough conditioning of the Tokamak will be required to remove Hydrogen contamination.

A Fokker-Planck calculation in these three situations has been performed [2] assuming an isotropic distribution, $T_e = T_i$ and $Z_{eff} = 1$. Figure 6 gives the fusion amplification factor $Q = P_{Fusion}/P_C$ versus P_C , the power effectively coupled to He³ in S1 and S3 scenarios or to the beam ions in the S2 scenario.

Scenario S1 appears to give the highest Q which reaches 0.06 for JET parameters with full ICRF heating. It is also the most effective scenario from the point of view of coupling to the desired species since the damping per pass is expected to be high ($\approx 70\%$) and no other competing damping (to H for instance) can occur. The Fokker-Planck code predicts that minority velocity distribution will become highly anisotropic with a "parallel temperature" ($T_{//}$) not exceeding 20 keV, which defines, from Doppler effects, an absorption layer of ± 30 cm. However, it is likely that a velocity space instability will relax the anisotropy, increase $T_{//}$ and broaden the deposition profiles.

The production of 16 MeV γ 's has already been observed in JET [10] in conditions corresponding to S1. The observed flux corresponds to about 15 kW of D-He³ fusion reaction power or to $Q \approx 3 \times 10^{-3}$. With $T_e \sim T_i \sim 5$ keV and $Z_{\text{eff}} \approx 2$, this value corresponds to $P_{\alpha} \sim 0.1$ MW m^{-3} which implies a deposition profile extending to $r = 0.6$ m. No attempt has yet been made to optimize the He³ concentration to reach the maximum Q value.

6. THE LOWER HYBRID CURRENT DRIVE PROJECT The large temperature collapses which are observed during sawteeth with high additional power deteriorates the fusion yield and can generate a locked MHD modes with a decrease of confinement time (-25%) and, in some cases can cause a major disruption. JET has proposed a Lower Hybrid Current Drive system in order to permanently stabilize the sawteeth. The main parameters are given in Table 1.

Table 1

Frequency	3.7 GHz	- Avoid coupling to NBI ions - Reach $n_0 = 10^{20} \text{ m}^{-3}$
$n_{//}$	$1.2 < n_{//} < 2.4$	48 multijunction units
Coupled Power	1.6 MW (stage 1),	10 MW (stage 2)
Current Drive	0.1 to 0.25 MA/MW, with $n_e = 5 \times 10^{19} \text{ m}^{-3}$	

The construction of Stage 1 has started and a prototype launcher is expected to be ready in mid 1988.

7. CONCLUSION The first stage of the JET ICRF heating programme has been completed and the main objectives have been achieved. Net coupled powers in excess of 7 MW, $T_{e0} = 7$ keV and $T_{i0} = 5.5$ keV have been obtained. The total radiated power is less than 25% of the input power when Helium conditioning is used.

Off-axis heating suggests that the heat transport is diffusive. On-axis heating is always more efficient and slows down, rather unexpectedly, the internal sawteeth relaxation. The quiescent period lasts no more than 1.6 s but has a beneficial effect on the fusion yield. The best incremental confinement time has been

obtained in X-point discharge although a transition to an H mode has not yet been observed.

The JET HF programme is being vigorously pursued with the upgrading of the ICRH to 20 MW with 8 antennae, the preparation of high fusion yield scenarios, and the development of a Lower Hybrid Current Drive system capable of driving up to 2.5 MA.

REFERENCES

- [1a] J. Jacquinet et al, Plasma Phys. and Contr. Fusion 28 1 (1986)
- [1b] J. Jacquinet et al, JET-P (86) 18, to be published in the Philosophical Transactions of the Royal Society
- [1c] JET team, "RF Heating on JET" 11th Int. Conf. on Plasma Physics and Controlled Fusion Research, IAEA-CN-47/F-I-1 (1986)
- [2] T. Hellsten, K. Appert, W. Core, H. Hamnén, S. Succi, Proc. of the 12th Eur. Conf. on Contr. Fusion and Plasma Phys. Budapest (1985)
- [3] M. Bures et al, accepted for publication in Plasma Physics and controlled Fusion
- [4] P.P. Lallia et al, Plasma Phys. and Conf. Fusion, 28 1211 (1986)
- [5] J.D. Callen, J.P. Christiansen, J.G. Cordey, P.R. Thomas, K. Thomsen, JET P (87) 10, submitted to Nuclear Fusion
- [6] P.H. Rebut, M. Brusati, M. Hugon, P.P. Lallia, 11th Int. Conf. on Plasma Physics and Cont. Fusion Research, IAEA-CN-47/E.III 4 (1986)
- [7] M. Brusati, private communication
- [8] V.P. Bhatnagar et al, to be presented at the EPS Conf. Madrid (1987)
- [9] D.F.H. Start et al, this conference
- [10] G. Sadler et al, to be presented at the EPS Conf. Madrid (1987)
- [11] G.A. Cottrell et al, this conference
- [12] B.J.D. Tubbing, N.J. Lopes Cardozo, JET-R(87)01.

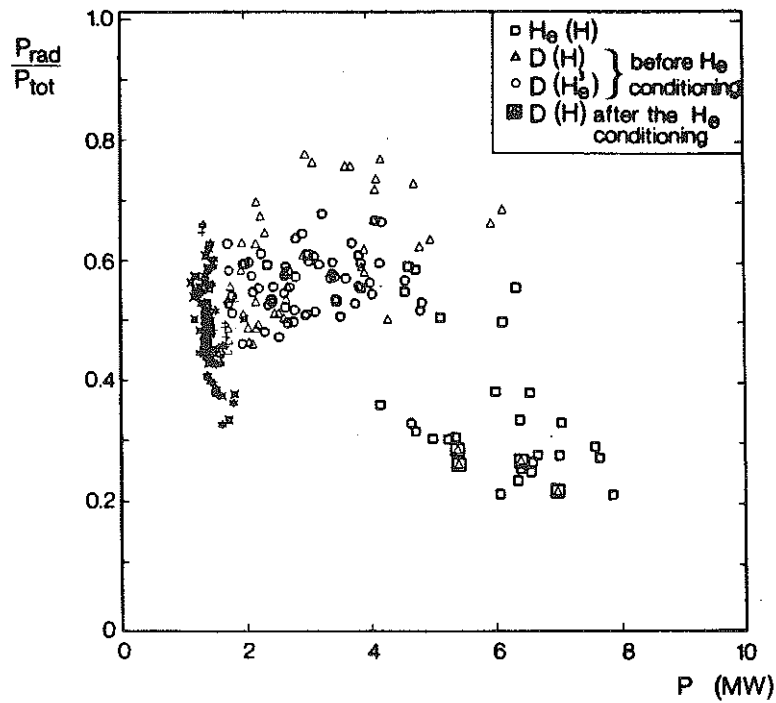


Fig. 1 Total radiated power normalised to the total input power (RF + ohmic) versus total input power. 2 MA discharges with $1 < n_o \times 10^{-19} < 2.5$

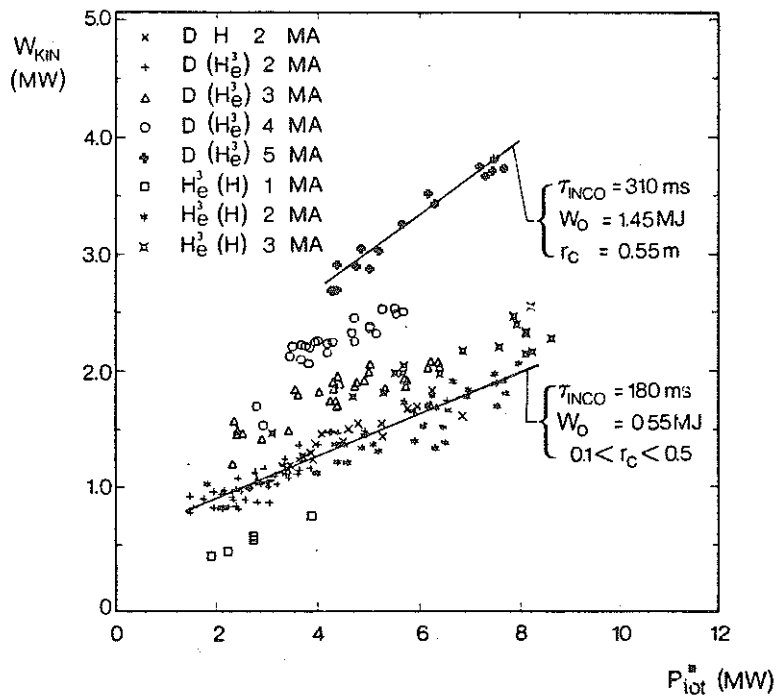


Fig. 2 Plasma stored energy versus effective input power $P_{tot}^* = 0.85 P_{OH} + (1 - \chi) P_{RF}$; $\chi = (R_c - R_o)/a$. In the diffusion heat transport model with constant $\chi(VT)$, the deposition of P_{tot}^* exactly on the magnetic axis produces the same increase of W than the distributed power P_{OH} and P_{RF} .

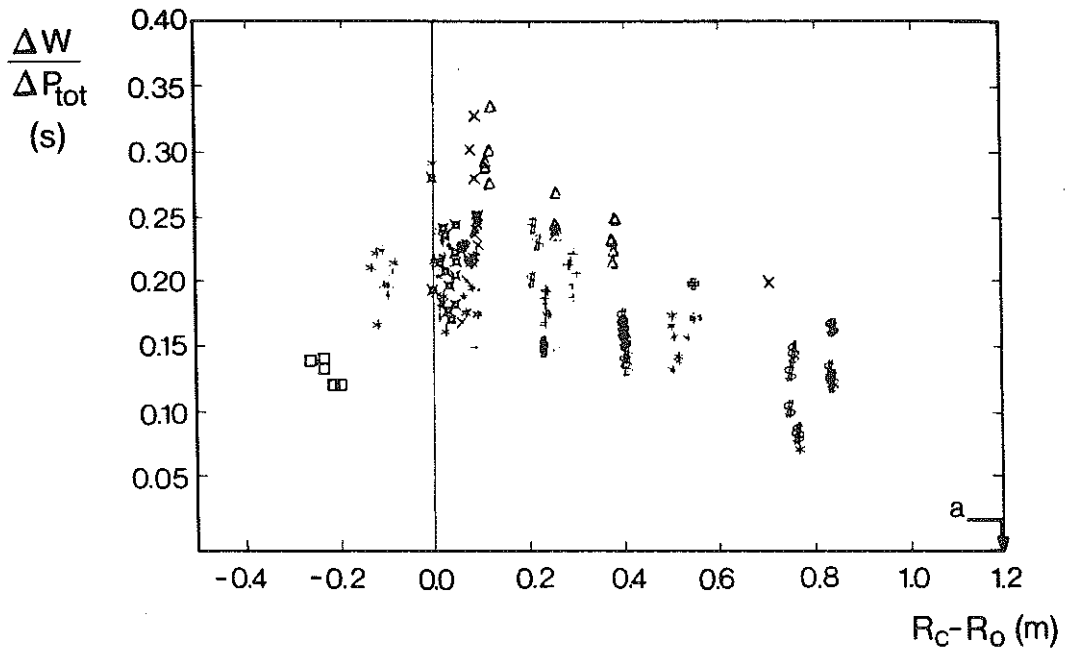


Fig. 3 Incremental confinement time $\Delta W/\Delta P_{\text{tot}}$ with $P_{\text{tot}} = P_{\text{OH}} + P_{\text{RF}}$ versus the position of the cyclotron resonance (R_C) with respect to the magnetic axis (R_0) for all JET limiter data. The symbols are explained on Fig. 2, in addition 2.5 MA data points are represented by \$. Note the general decrease of the heating efficiency with off-axis heating which can be represented by a law $(1 - \chi)$

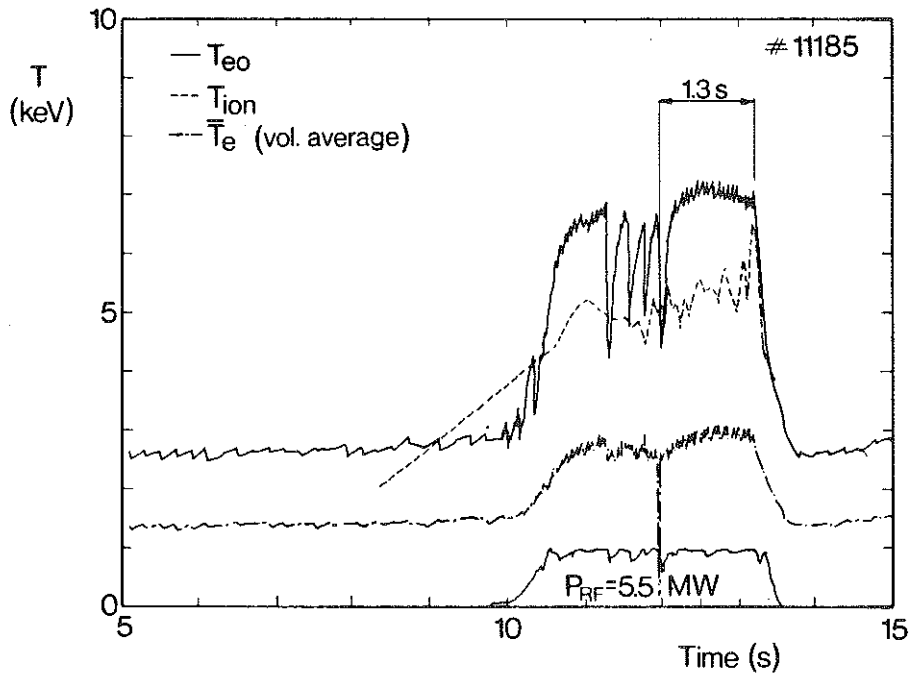


Fig. 4 Evolution of the electron and ion temperatures during 5.5 MW heating pulse (3.5 sec) in an X-point discharge (Helium plasma). 2 monster sawteeth are separated by normal sawteeth.

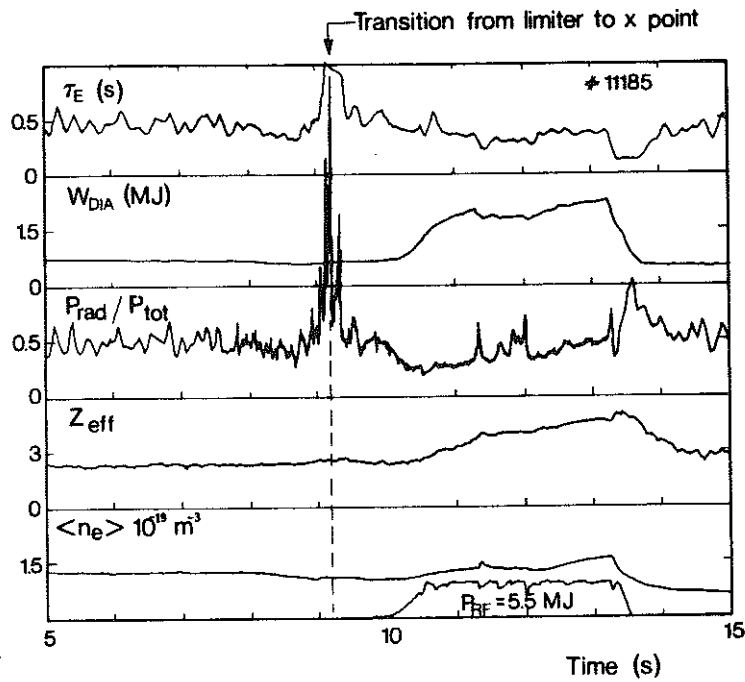


Fig. 5 Evolution of plasma parameters during a 5.5 MW heating pulse in an X-point discharge. Note the increase of density and stored energy during the monster sawtooth. The high Z_{eff} and $P_{\text{rad}}/P_{\text{tot}}$ is typical of the high power X-point discharge.

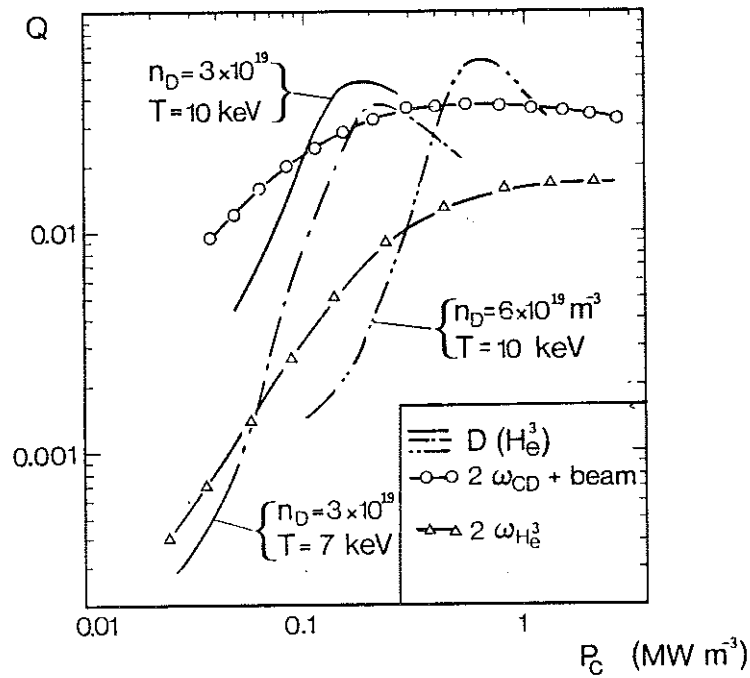


Fig. 6 Fusion amplification factor for D-He³ reaction versus the power damped in the resonating species. 3 scenarios are considered (i) D(He³), He³ resonating minority with $n_{\text{He}^3}/n_{\text{D}} = 0.02$ (ii) $2\omega_{\text{CD}}$, Harmonic resonance with Deuterium beam ions, $E_{\text{inj}} = 80$ keV, $n_{\text{He}^3}/n_{\text{D}} = 1$ (iii) $2\omega_{\text{C He}^3}$, Harmonic resonance with Helium3, $n_{\text{He}^3}/n_{\text{D}} = 0.5$. In all cases $Z_{\text{eff}} = 1$